3-1-2018

Pilot ambient noise tomography study for mineral exploration potential

Sheri Molnar
The University of Western Ontario, smolnar8@uwo.ca

Hema Sharma
Western University, hsharm3@uwo.ca

Western Science

Pilot ambient noise tomography study for mineral exploration potential

For
Stillwater Canada Inc.
90 Peninsula Road, Marathon, Ontario, Canada, P0T 2E0

By
Hema Sharma and Dr. Sheri Molnar
Department of Earth Sciences, Western University
London, ON, Canada

NSERC CRSNG
Natural Sciences and Engineering Research Council of Canada
Conseil de recherches en sciences naturelles et en génie du Canada
Canada

MARCH 1, 2018

Table of Contents

List of Figures

Introduction

This report describes the analysis of ambient vibration data collected from 31 sites in Marathon, ON, Canada, using 31 vertical component geophones (Figure 1). The Eastern Gabbro Suite comprises the Marathon deposits of platinum group metals and copper.

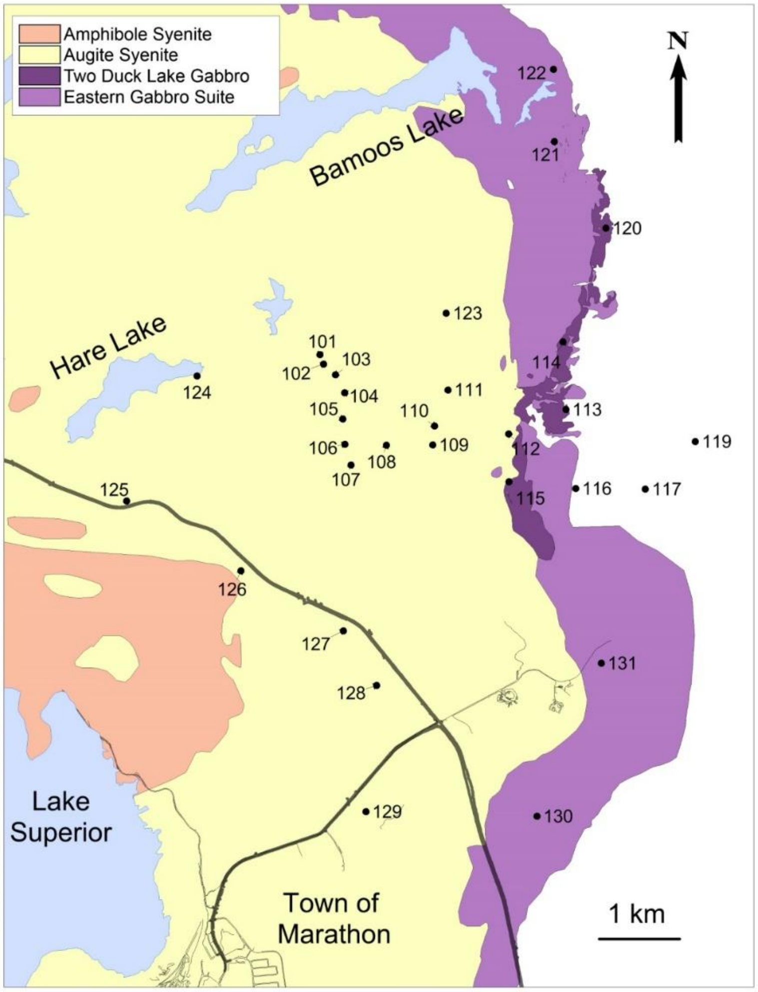

Figure 1. Geological map of Marathon showing the geophone sites (modified from EcoMetrix Report, 2012).

The survey for ambient noise data collection was conducted over a period of 31 days, starting at 3 pm on 10th September and ending at 8 am on 10th October 2017. However, data could not be recorded for all the 31 days at a few sites due to technical issues with the geophones. Data could only be recorded for 19 and 20 days for site 110 and 116 respectively, and for 26 days each for site 121 and 128. Data were given to the Western University in miniSEED format in the last week of January 2018. Data were examined for time-frequency analysis, to understand the effect of wind speed on the ambient vibration data, and to estimate subsurface shear wave velocity by Rayleigh wave dispersion curve inversion.

Methodology & Results

Time-frequency analysis

Data for three sites were analysed for all days and converted from time domain to frequency domain. The three chosen sites are: 128, which is near the Marathon Airport and Lake Superior; 112, which is centrally located in the array and about 200 m away from the road; and 122, which is farthest from the Lake Superior and the airport and is about 50 m away from the road (Figure 2a). Figure 2b to 2d show the amplitude variation with high frequency (1-25 Hz) for these three sites. Since site 128 is closest to the airport, we can see a large amplitude at high frequencies (Figure 2b). As we move away from the airport towards sites 112 and 122, the amplitude decreases drastically, as seen in Figure 2c and 2d. Since site 122 is closer to the road, it shows relatively higher amplitude due to the road traffic in comparison to site 112. The high amplitudes for site 128 are localised around 15 Hz. The amplitudes for site 112 are mostly of uniform lower intensity due to continuous background noise. The distribution of high amplitudes for site 122 is quite sparse and is higher probably when the road traffic is more.

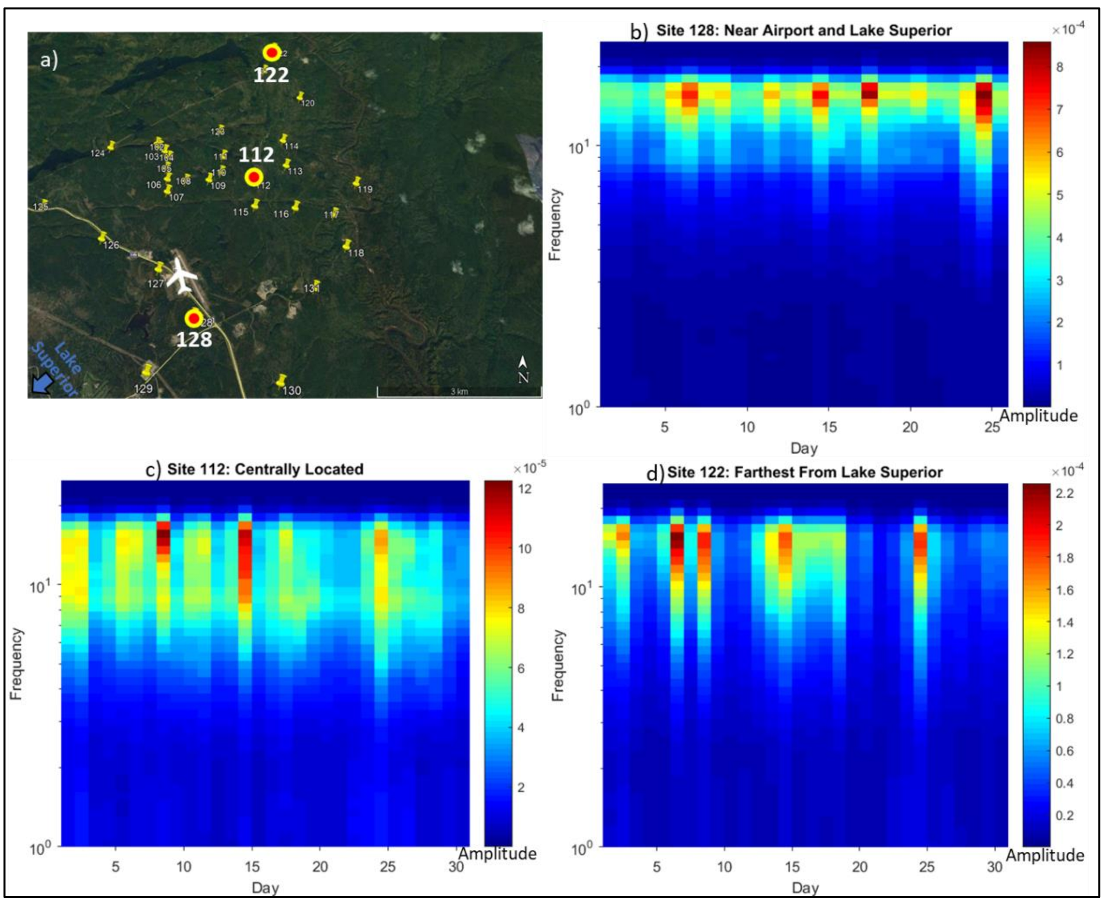

Figure 2. (a) Map showing the three studied sites (128, 112, and 122). Also shown are the high frequency (1-25 Hz) spectrum for (b) site 128 showing higher amplitudes due to airport proximity, (c) site 112 showing uniform background noise, and (d) site 122 showing sporadic higher amplitude peaks due to road traffic.

Figure 3b to 3d show the low frequency response at the three sites. The distribution of low frequency amplitudes for all the three sites are almost same, with the amplitudes for 128 being slightly higher due to its proximity to the Lake Superior, which is approximately 3.4 km SW of the site. The higher amplitudes seen at each site can be explained by strong wind conditions on certain days. The wind data are shown in the following section.

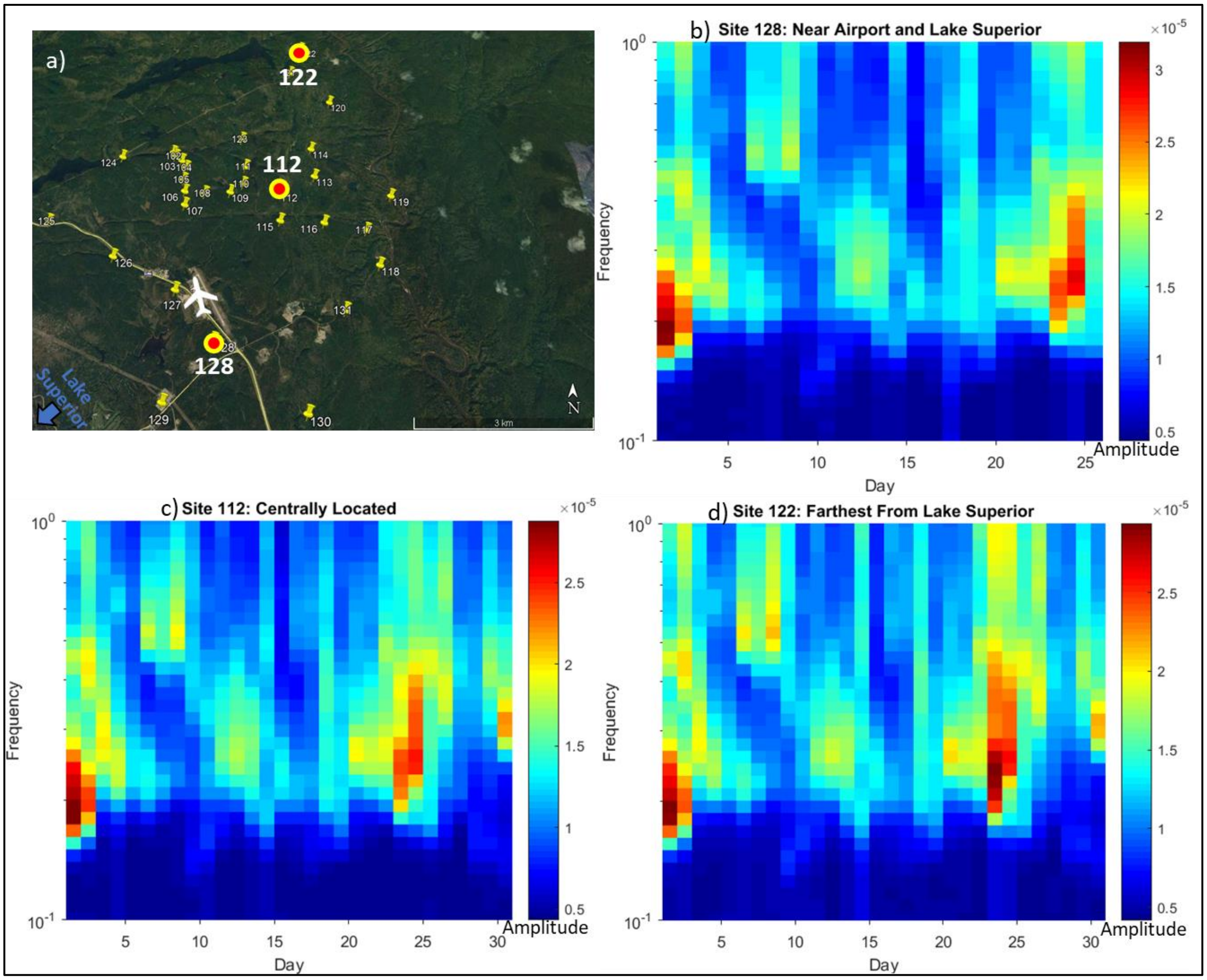

Figure 3. (a) Map showing the three studied sites (128, 112, and 122). Also shown are the low frequency (0.1-1 Hz) spectrum for site 128 showing slightly higher amplitudes due to its proximity to the Lake Superior (b), sites 128, 112 and 122 show similar amplitude distribution at these frequencies (b, c, and d respectively). Higher amplitudes at each of these sites correspond to days with strong winds.

Amplitude variation with wind speed and direction

The variation of amplitude with wind speed was also studied. Figure 4a shows the location of two stations: Lake Superior buoy and Marathon Airport land station, where the weather data is continuously measured by Environment Canada. The wind speed at these locations were obtained for the same time interval of

study and averaged for each day (Figure 4b). Although the average wind speed at the Lake Superior buoy is higher than that at the Marathon Airport, their temporal variation is mimicking each other. Since Marathon Airport land station is closer to the sites, we have taken wind speed measurements at this station.

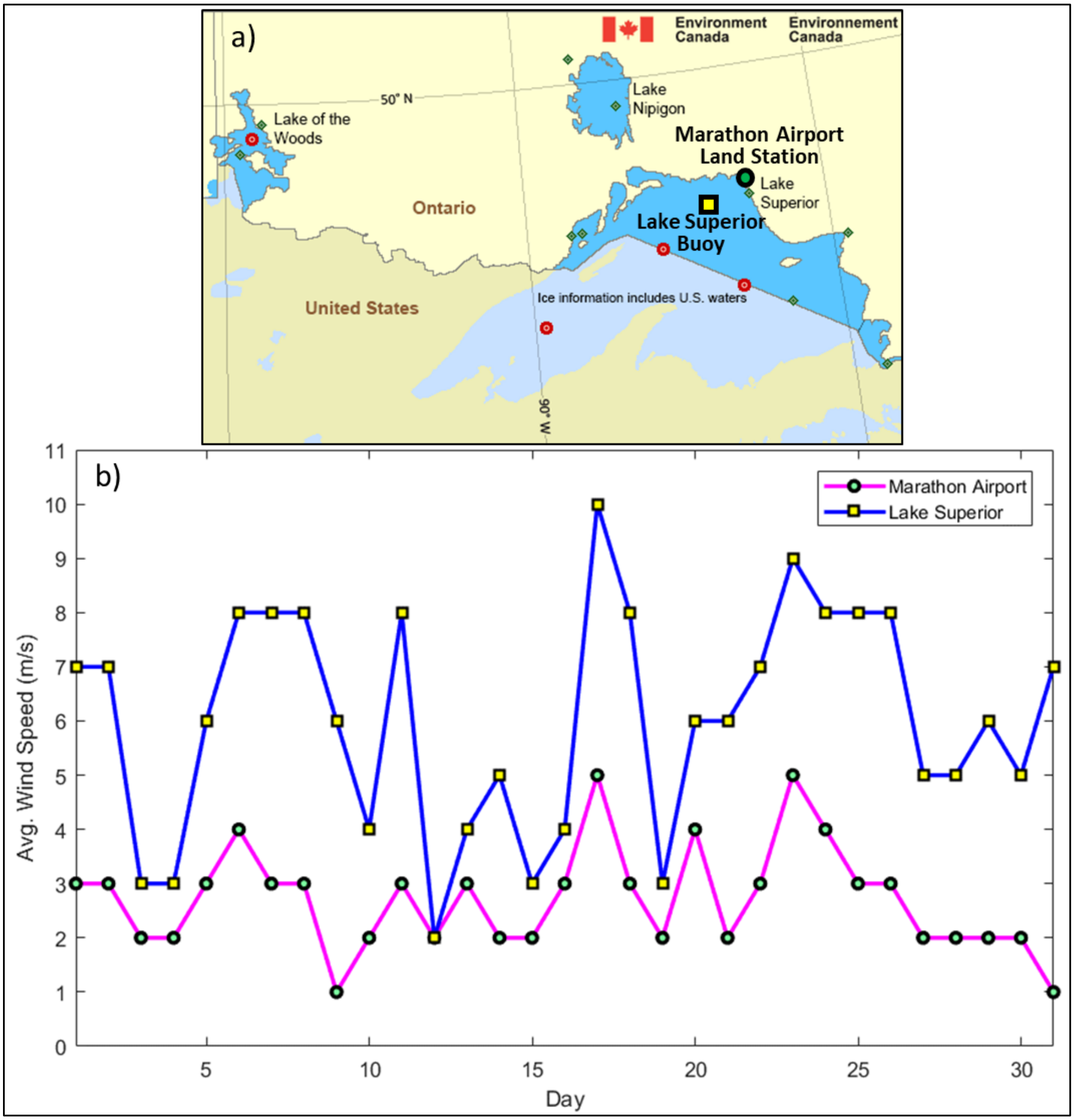

Figure 4. (a) Location of Lake Superior buoy and Marathon Airport land station where wind speeds are continuously measured; (b) Average wind speed (m/s) per day for 31 days from 10th September to 10th October. Variation in average wind speed is consistent at the two locations. However, the average wind speed at the Lake Superior is higher.

Figure 5b to 5d show the amplitude variation w.r.t. the wind speed at high frequencies. The amplitudes at higher wind speeds are generally higher and are generally lower at lower wind speeds. As mentioned in the

previous section, the amplitudes at high frequency are being affected by the airport and road traffic at sites 128 and 122 respectively.

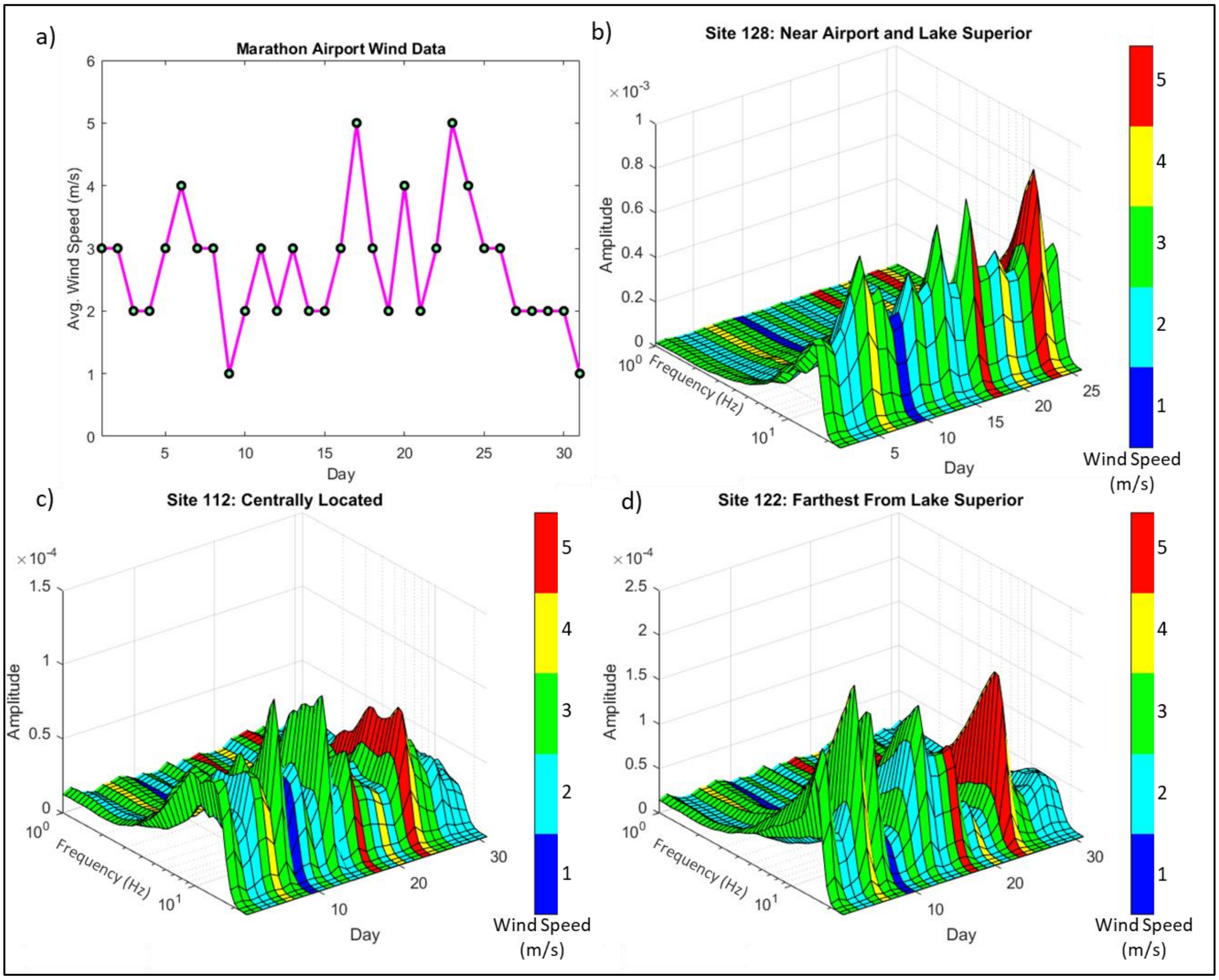

Figure 5. (a) Daily average wind speed measured at Marathon Airport land station. Amplitudes at high frequency (1-25 Hz) for each day at site 128 (b), 112 (c), and 122 (d).

The variation of amplitude at lower frequency w.r.t. wind speed is shown in Figure 6b to 6d. The higher amplitudes at each site correspond to higher average wind speed. However, on day 17 when the wind speed was high (5 m/s) the amplitudes are low. This could be because these winds were coming from ENE and not from the direction of Lake Superior and hence the waves from the Lake Superior were not affecting the low frequency amplitudes. On the other hand, on day 23, the wind is coming from the general direction of the lake (from south). Hence, the wave action of the lake is affecting the low frequency amplitudes.

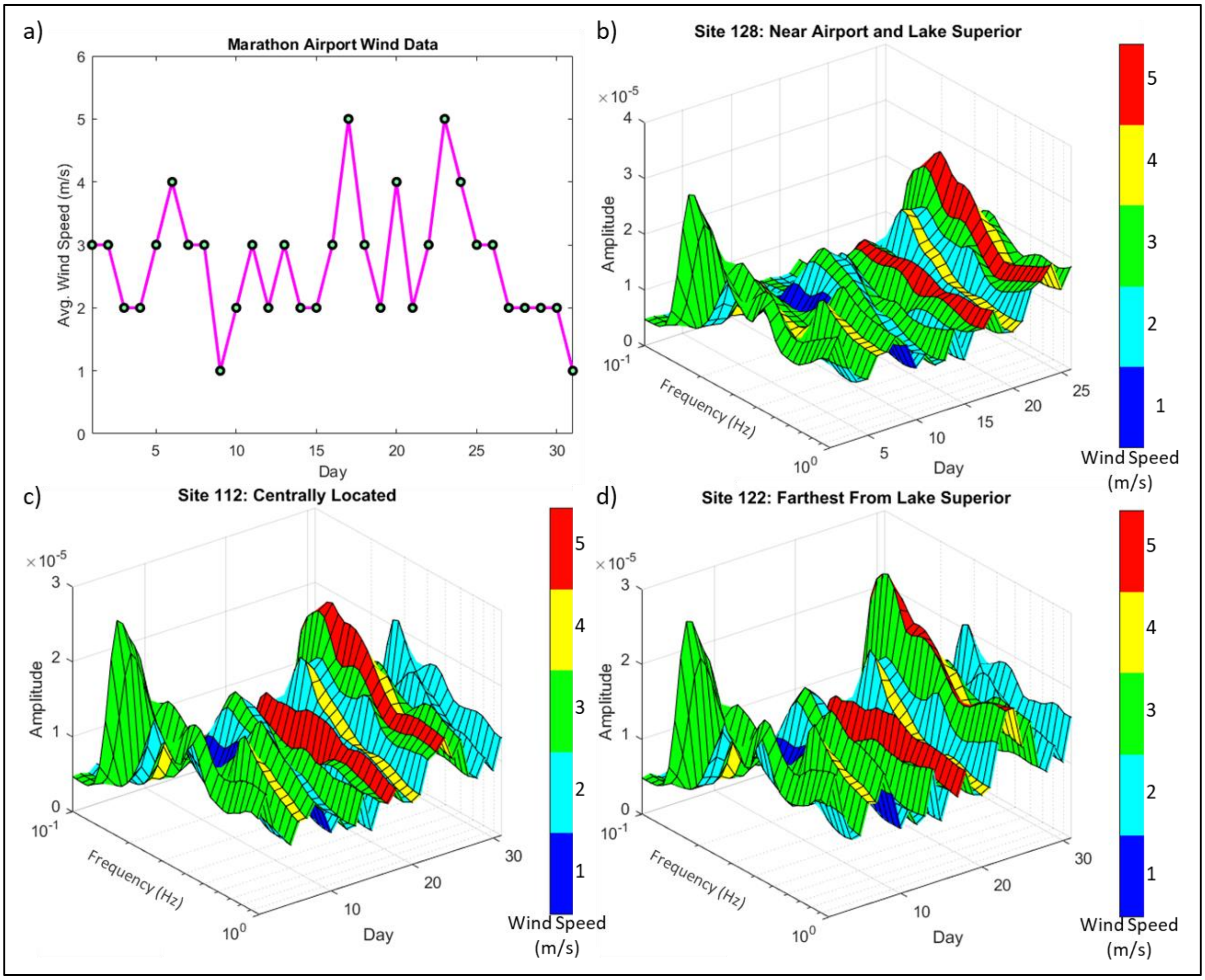

Figure 6. (a) Daily average wind speed measured at Marathon Airport land station. Amplitudes at low frequency (0.1-1 Hz) for each day at site 128 (b), 112 (c), and 122 (d), show higher values at higher wind speed, except for day 17. Please see text for details.

19 sites were chosen scattered throughout the study area to examine the relationship between average wind speed and amplitude. We chose a very calm day and a very windy day based on the above data for amplitude vs. wind speed analysis. Day 9 (18^{th} September) was chosen as the calm day since all the sites have data for this day and the wind speed is also lowest at 1 m/s. The average wind direction for this day is SW. Similarly, 2^{nd} October or day 23 was chosen for a very windy day for it had highest wind speed of 5 m/s and coming from the direction of the Lake Superior. Figure 7 shows the average amplitudes for these two days at low (0.1-1 Hz) and high (1-25 Hz) frequency intervals.

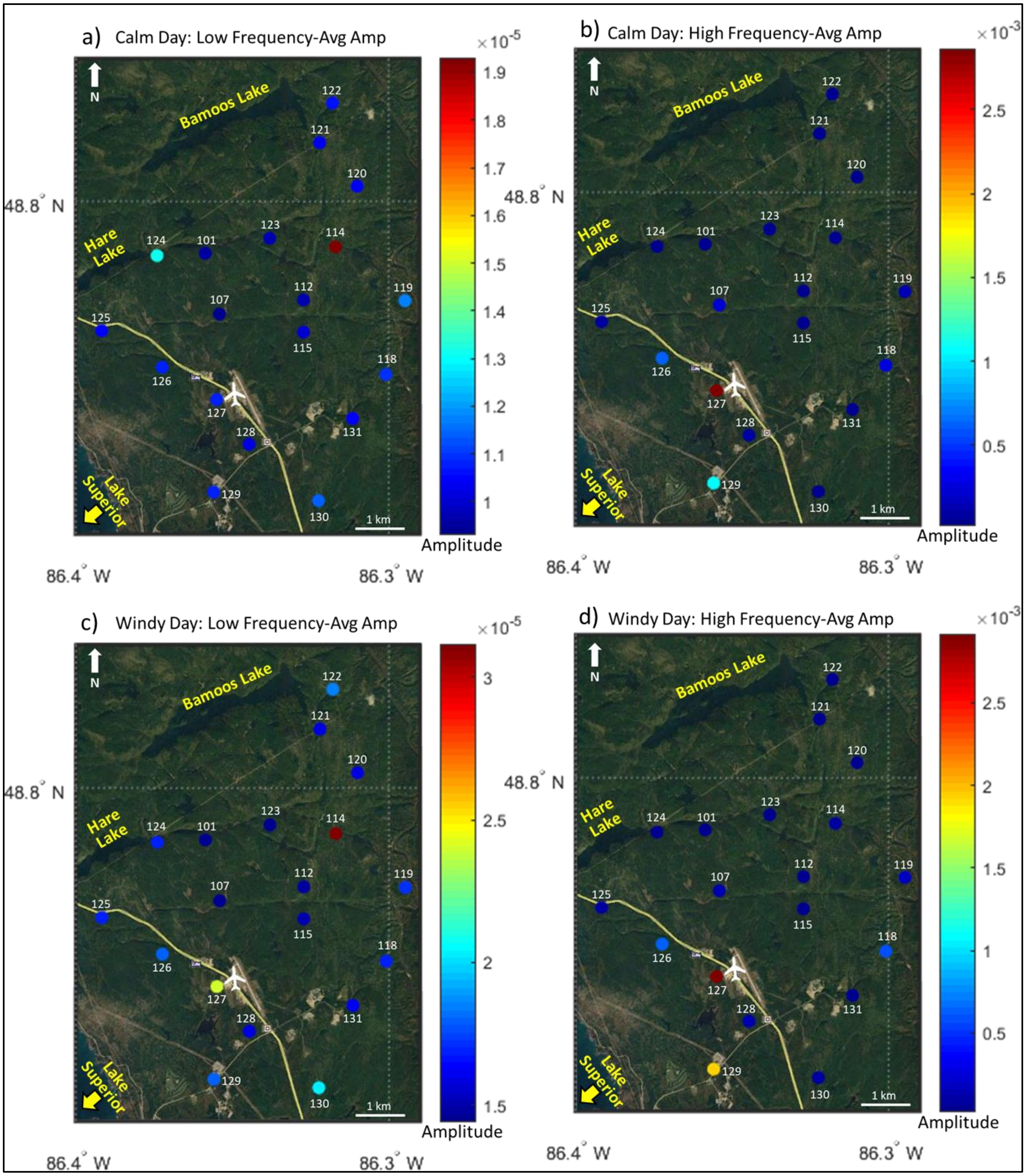

Figure 7. Average amplitudes for calm (9th day) (a and b) and windy (23rd day) (c and d) day for lower (0.1-1 Hz) and higher (1-25 Hz) frequencies respectively.

At low frequencies, the average amplitudes for all the 19 sites are higher on the windy day (Figure 7a and 7c). On the other hand, at high frequencies, amplitudes are in the same range for both calm and windy day. However, exception to this observation can be seen at two sites, 114 and 124 (Figure 7a and 7c). We posit

that the proximity of site 124 to the Hare Lake may have influenced the amplitudes at low frequencies. Whereas, site 114 has very high low frequency amplitudes for both the calm and windy day which may be because of long-period waves coming from the Lake Superior or due to some technical issues with the data recording. The spectra of these two sites at low frequency bandwidth is also different from the other sites in terms of the peak observed at low frequencies. For these two sites, especially for site 114, a sharp low frequency peak was observed at about 0.5 Hz, while this was not the case for the other sites.

Also, the low frequency amplitudes for sites 127 and 130 are higher on windy day. This is probably due to the wave action from Lake Superior.

Shear wave velocity (V_S) estimation

To estimate $V_{S,}$ four arrays were designed, as shown in Figure 8.

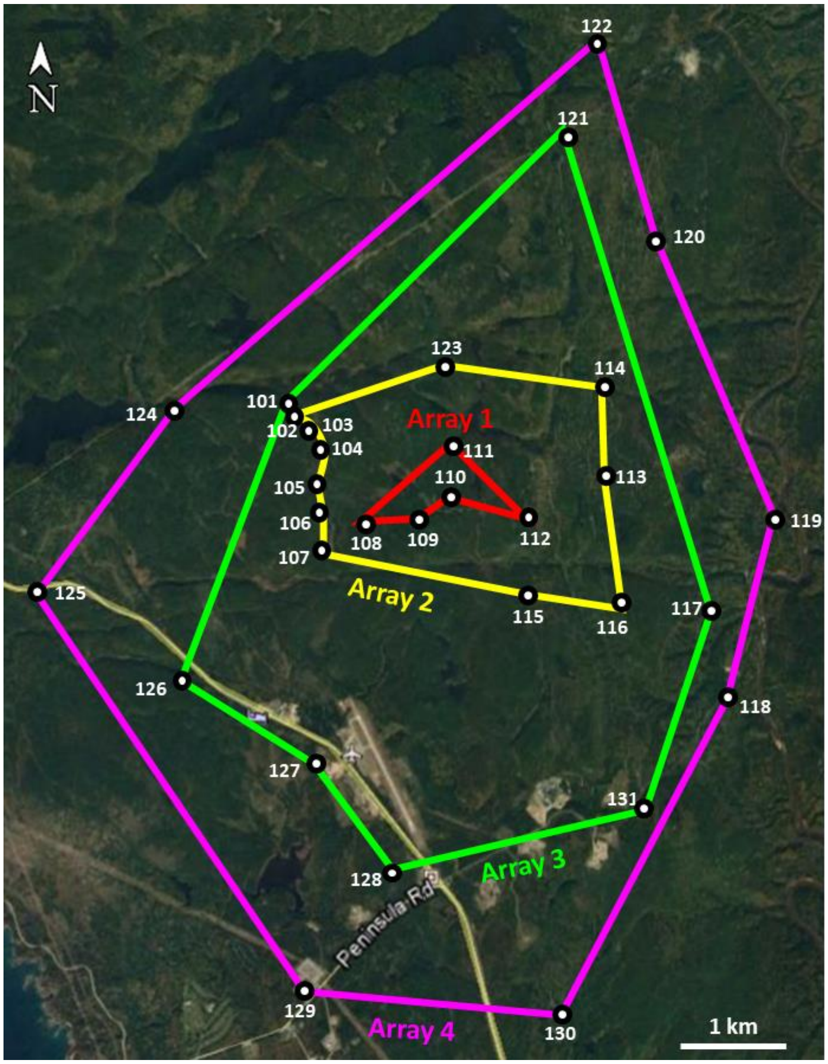

Figure 8. Four arrays (Array 1, 2, 3, and 4) designed from the sensor distribution.

These arrays were designed to obtain a dispersion curve for a wider frequency range. For dispersion curve analysis, data for day 4 (13th September), from 12am to 4am were processed using high resolution frequency-wavenumber (HRFK) method. The velocity histograms obtained after HRFK are shown in Figure 9. Also shown is the picked dispersion curve using velocity histograms.

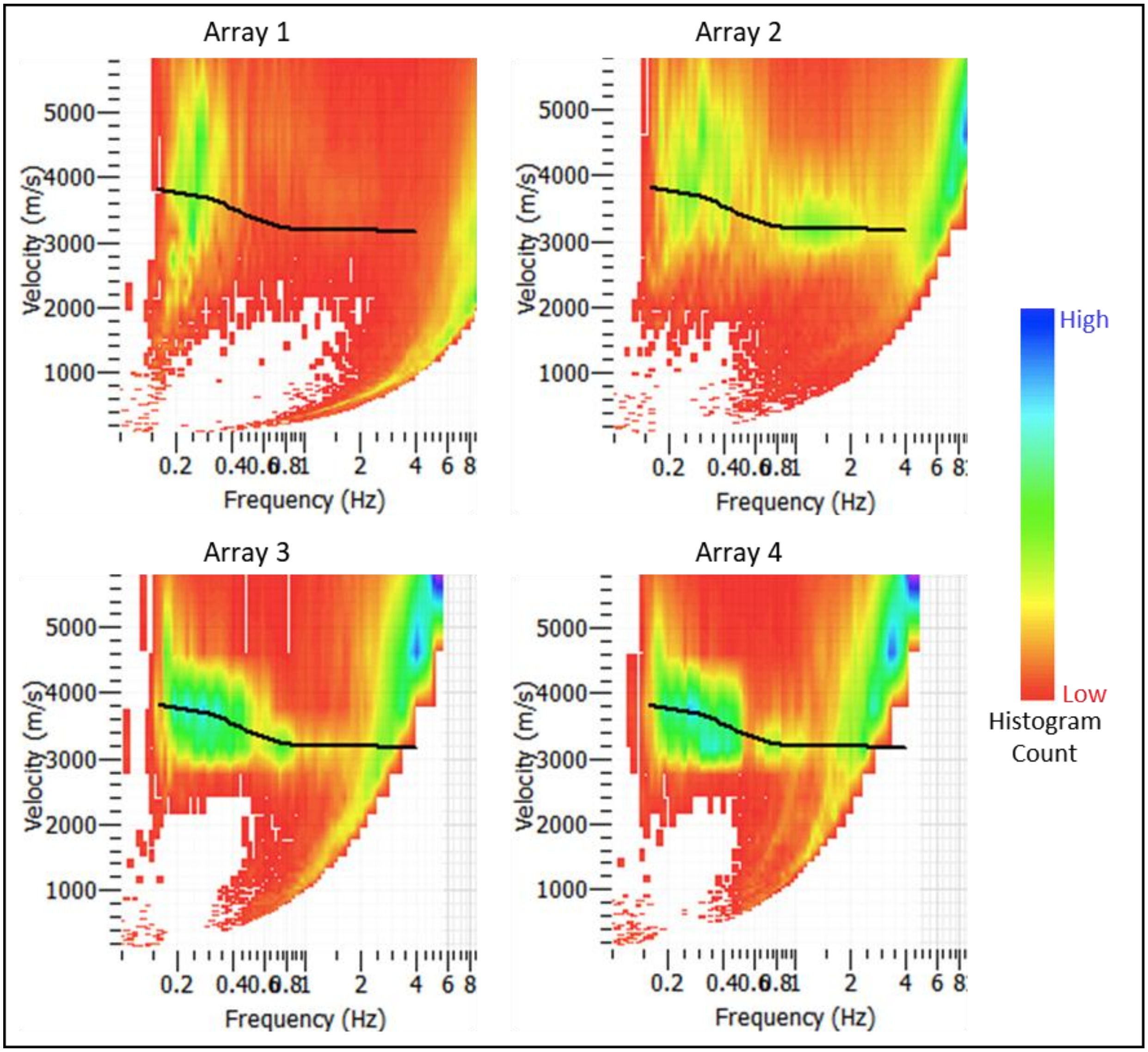

Figure 9. Picked dispersion curve overlaid on velocity histograms for different arrays. The same dispersion curve was utilized for V_S estimation.

We were able to pick only the fundamental mode dispersion curve for Rayleigh wave velocity spectra. Since Array 1 was not very helpful in picking the dispersion curve, velocity histograms obtained for Array 2, 3, and 4 were used to pick the dispersion curve. The dispersion curve was manually picked from ~0.16 to ~4.3 Hz. Since this is a hard-rock site, velocity histograms have limited resolution at lower frequencies

(<0.5 Hz) resulting in widely distributed higher histogram counts. This affected the certainty in dispersion curve picking. This dispersion curve was then inverted to obtain a V_S depth profile as shown in Figure 10a.

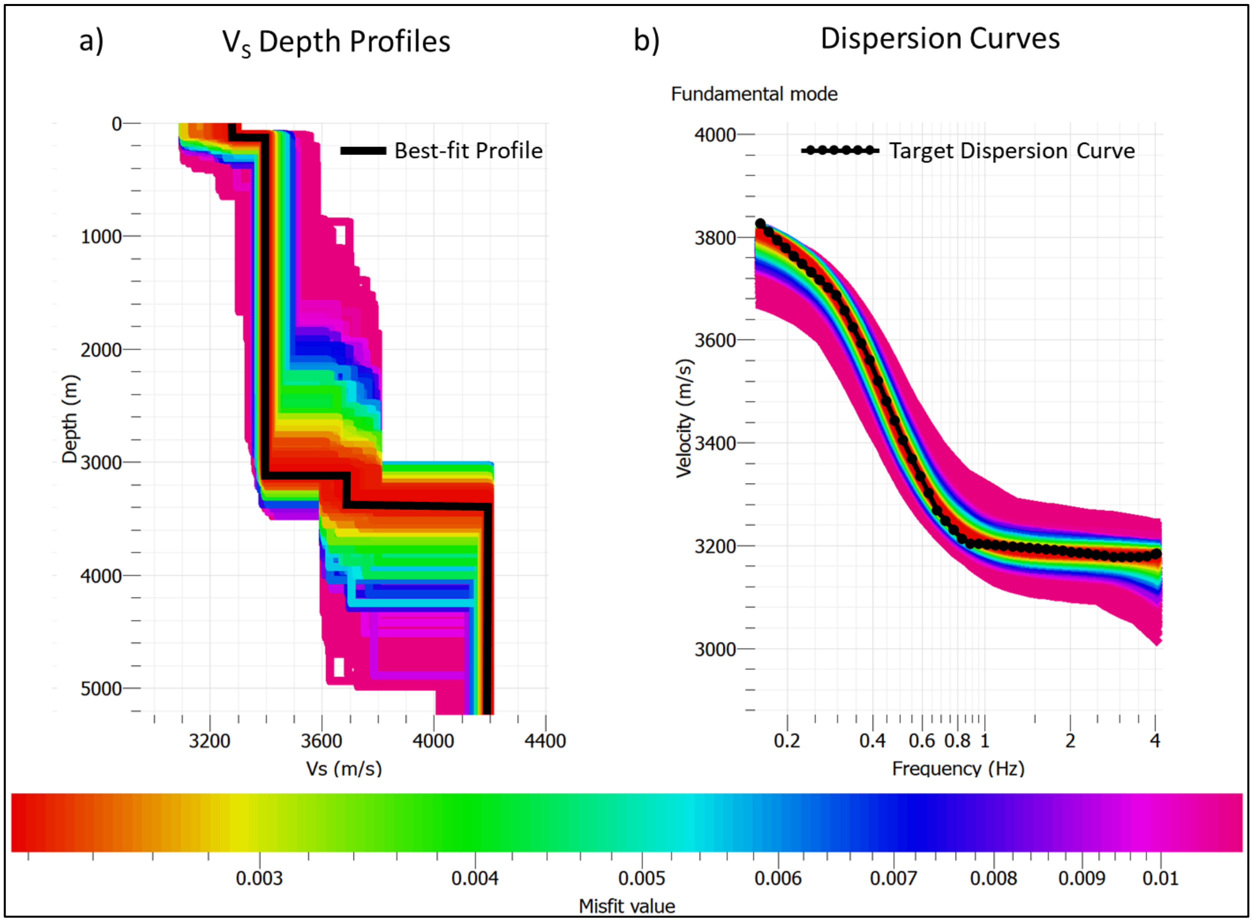

Figure 10. (a) Best-fitting V_S profile is shown in black and a set of tested velocity profiles that are colored according to the misfit value; (b) Target dispersion curve in black, also shown are the forward modeled dispersion curves colored according to their misfit values.

Figure 10a shows the best-fit V_S profile in black color. As the depth increases V_S also increases. The target dispersion curve is shown in black color in Figure 10b. The inverted fundamental mode Rayleigh wave dispersion curve for the best-fit model matches very well with the target dispersion curve.

Spatial distribution of Rayleigh wave velocity

We designed three different areas for spatially varying Rayleigh wave velocity (Figure 11). As mentioned in the Seisprobe report, Area A has slightly lower velocity than Area B and C, due to the presence of the Eastern Gabbro Suite around Area B and C.

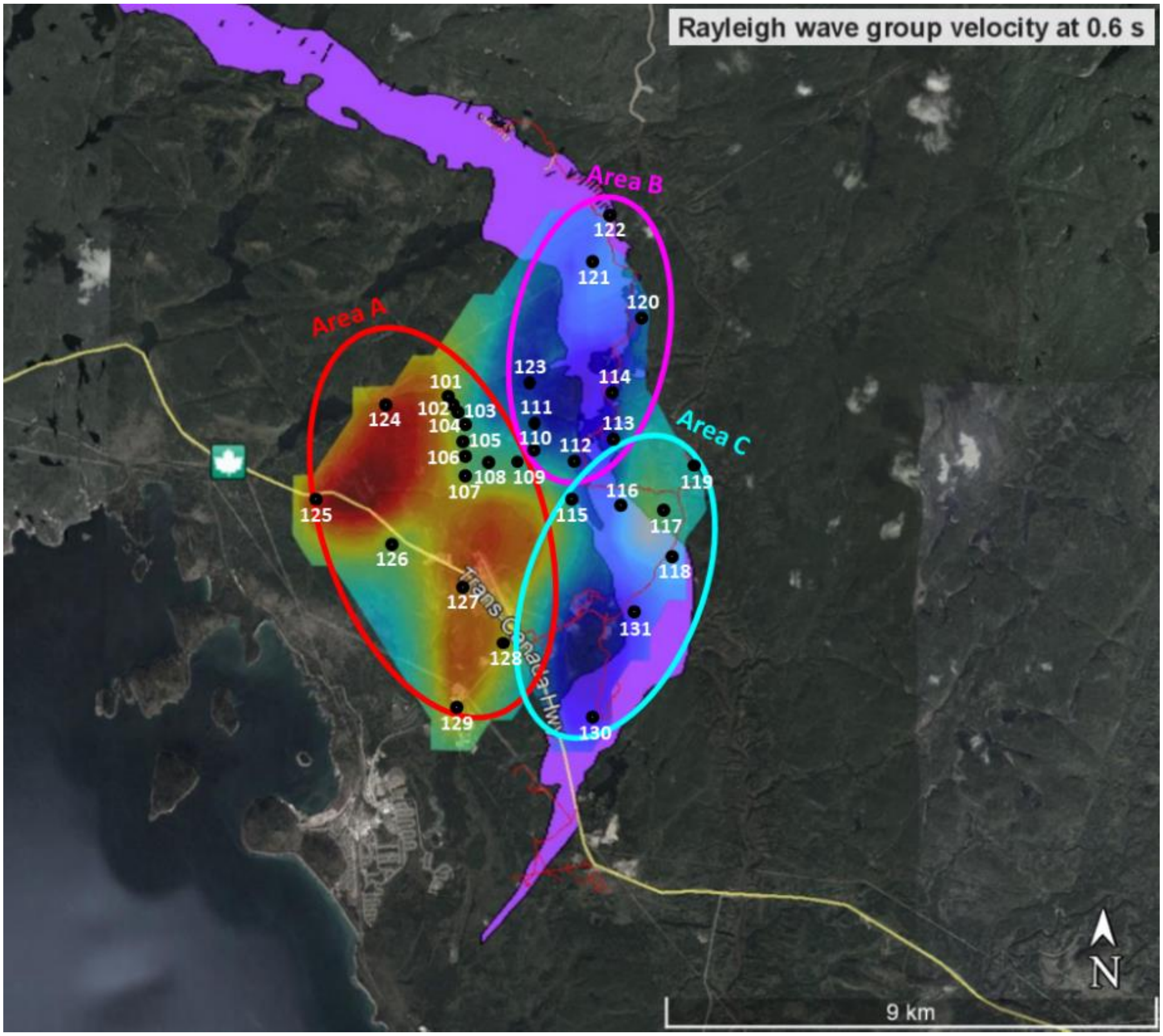

Figure 11. Area A, B, and C overlaid on the Rayleigh wave group velocity surface at 0.6 s (from Seisprobe report).

HRFK analysis was carried out to obtain Rayleigh wave velocity histograms for these three regions (Figure 12). The Rayleigh wave velocity spectra show that all the three areas have relatively similar velocity values. The spread of the high histogram count is wide for all the three spectra due to low data resolution. We expect that a denser data acquisition may lead to higher resolution, especially at higher frequencies (>1 Hz). This will also reduce the uncertainty in picking the dispersion curves.

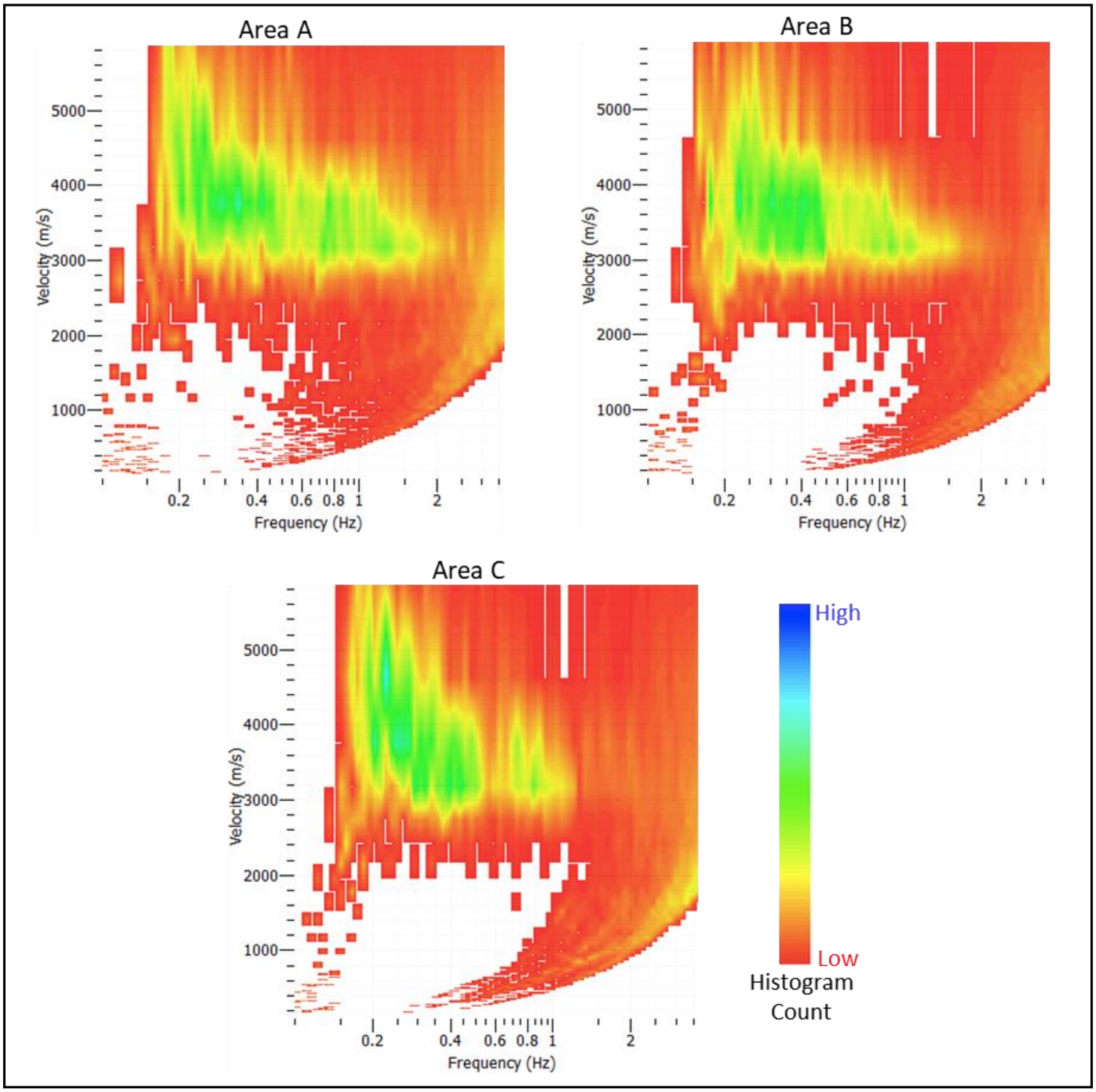

Figure 12. Rayleigh wave velocity spectra for Area A, B, and C. Wide scatter of higher velocity counts reflect low data resolution.

Conclusions

This study concludes that the high frequency amplitudes are mostly affected by the anthropogenic sources while the low frequency amplitudes are affected by natural causes including wind speed and direction and waves. The sites closer to the Lake Superior show higher amplitudes on windy day than on a calm day. Being a hard-rock site, the shear wave velocities is relatively high, in the range of 3100-4000 m/s. This makes dispersion curve analysis and inversion more challenging. Acquisition of denser data may improve the quality of the results.

Acknowledgements

This research was funded by the Natural Sciences and Engineering Research Council of Canada (NSERC: EGP 514509 - 17). We would like to thank Melanie Postman and Mark Novakovic for the data collection.